A numerical study on the softening process of iron ore particles in the cohesive zone of an experimental blast furnace using a coupled CFD-DEM method

Mehdi Baniasadi, Maryam Baniasadi, Gabriele Pozzetti, Bernhard Peters University of Luxembourg, Faculty of Science, Technology and Communication, 2, Avenue de l'Universit, L-4365 Esch-sur-Alzette, Luxembourg.

Abstract

Reduced iron-bearing materials start softening in the cohesive zone of a blast furnace due to the high temperature and the weight of the burden above. Softening process causes a reduction of void space between particles. As a result, the pressure drop and gas flow change remarkably in this particular zone. As a consequence, it has a significant influence on the performance of a blast furnace and is needed to be fully characterized. For this reason, the gas rheology along with the deformation of the particles and the heat transfer between particle-particle and particle-gas should be adequately described. In this paper, the eXtended Discrete Element Method (XDEM), as a CFD-DEM approach coupled with the heat transfer, is applied to model complex gassolid flow during the softening process of pre-reduced iron ore pellets in an Experimental Blast Furnace (EBF). The particle deformation, displacement, temperature, and gas pressure drop and flow under conditions relevant to the EBF operations are examined. Moreover, to accurately capture the high

gas velocity inlet, a dual-grid multi-scale approach is applied. The approach and findings are helpful to understand the effect of the softening process on the pressure drop and gas flow in the cohesive zone of the blast furnace. Keywords: XDEM, CFD-DEM, softening, heat transfer, iron ore pellet, cohesive zone

1. Introduction

A blast furnace (BF) is a complex chemical reactor by which iron is produced from iron-bearing materials. The BF is charged from the top with alternating layers of iron-bearing materials and coke descending downward by the gravity force. A high-velocity stream of preheated air is introduced through the tuyeres in the lower part of the BF to react with the coke. As a consequence, a counter-current flow of reducing gas, carbon monoxide (CO), that heats up and reduces iron-bearing materials in the shaft, is formed. Then, the reduced iron-bearing materials undergo softening and melting in the middle of the BF due to two main reasons: the load of the burden above and the high gas temperature. The latter changes the mechanical properties of the particle and the former promotes particles' compression. On the other hand, coke particles do not exhibit observable deformation. The region, where these phenomena take place, is usually referred to as cohesive zone (CZ) as illustrated in Figure 1 [1]. As the iron-bearing materials are softened and melted, the local void fraction decreases. This markedly reduces the permeability of the layers of iron-bearing materials, affecting the flow

distribution and, therefore, the convective heat transfer and temperature distribution. This complex set of mutual interactions between the gas and the discrete phases determines the main CZ features such as its thickness and position in the BF, which are known to have a profound effect on the production capability [2]. Therefore, the description of the characteristics of the softening and melting phenomena is essential for constructing a precise blast furnace model. Since it is often not possible to interrupt the BF to investigate details of the phenomena occurring inside via purely experimental studies, the numerical simulations can be a practical tool to approach those phenomena. In this contribution, we propose a numerical model that aims to study the softening process.

Continuum-continuum modeling has been used to describe the phenomena inside the blast furnace [3, 4, 5]. However, the continuum-continuum method cannot provide some significant information such as deformation and temperature of each particle, as well as the local void space between particles which are important, particularly, in the CZ modeling. As a result, the effects of those on the softening-melting process and the gas flow by those methods are ignored. Alternatively, Lagrangian-continuum numerical models can overcome these shortages. Computational fluid dynamics (CFD) and discrete element method (DEM) as a Lagrangian-continuum method has been used to simulate the conditions within the raceway or the shaft of the BF [6, 7, 8]. Moreover, this approach has been applied to model the whole BF considering the phenomena taking place in the CZ with several

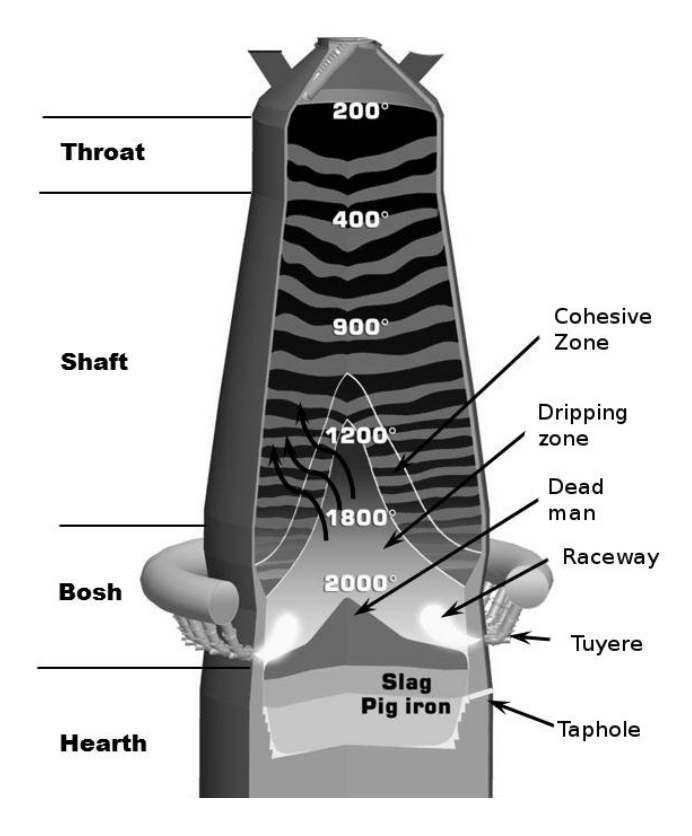


Figure 1: Sc1hematic diagram of different parts of blast furnace [1].

simplifying assumptions. For instance, Ueda et al. [9] used the CFD-DEM method to investigate the gas and solid flow in the different cohesive zone shapes by assuming that the iron ore layers are impenetrable. Kurosawa et al. [10] modeled the BF by considering the softening behaviour of particles due to load within the cohesive zone. In [10], the ore particles are allowed overlapping thus reducing the void fraction of the bed and influencing the gas flow due to their softening. A three-dimensional model was adopted by Yang et al. [11] to examine the gas-solid flow in a BF with and without the CZ. However, heat transfer was not included in these works. Nevertheless,

an accurate solution of the temperature distributions for gas and particles are mandatory to predict the softening process correctly and therefore the characteristic of the CZ.

The deformation of a particle is caused by the change of the the Young's modulus, which is strongly dependent on particle temperature. As the temperature varies along the blast furnace, the properties of ore particles alter. Therefore, the assumption on the constant mechanical properties, particularly, Young's modulus in each part of the BF as was considered in [10] is not realistic. Recently, Yang et al. [12, 13] implemented temperature dependency of Young's modulus into DEM based on the experimental data carried out by Chew and Zulli [14]. The particle deformation, temperature, and gas pressure were examined in the softening and melting of wax balls. Baniasadi et al. [15] investigated the softening process of a type of iron ore pellet experimentally and numerically in a small scale. However, the gas rheology was not considered in this study. To date, there is no research on the simulation of the softening behaviour of the iron-bearing particles along with the gas rheology changes and heat transfer in a large scale.

As mentioned, the hot gas is introduced from tuyeres and react with coke to produce the reducing gas. This gas flowing upward carries out some vital functions such as to heat up the particles, to reduce iron-bearing materials, and to melt reduced iron ore particles in different parts of a BF. Therefore, an accurate prediction of the fluid dynamic is mandatory to predict not only particle softening but also the whole BF process correctly. However, obtaining

accurate and grid-convergent solutions for the fluid flow within CFD-DEM couplings is a challenging task. As shown by Pozetti et al. [16], the nature of the volume averaged coupling between CFD and DEM domains can force researchers to use coarse-grids for the fluid solutions that do not allow resolving fine-scale fluid structures. This can lead to solutions that cannot ensure grid-convergence nor accuracy. For the BF modeling, this issue can significantly affect the ability to reconstruct the high-velocity gas flow [6]. In particular, in [6], the fundamental role played by the inlet condition on the fluid-dynamic behaviour of the BF was proven; still, the numerical experiments were limited to very-low velocities. For this reason, we here adopt the dual-grid multiscale approach initially introduced in [16] that allows us obtaining detailed information on the high-velocity flow field and in particular on its temperature distribution. This ultimately leads to a more reliable evaluation of the heat transfer between fluid and particles.

In this contribution, the eXtended Discrete Element Method (XDEM) [17], which is a multiscale and multiphysics numerical simulation method is used to model the softening process of iron ore pellets in the CZ of an EBF. The XDEM is a CFD-DEM method with some extra features such as heat transfer coupling and dual-grid multiscale approach. The XDEM has been applied to different phenomena taking place in the blast furnace. In particular, it has been validated for the heat up and reduction of iron ore pellets in the shaft [18, 19], and the flow behavior of molten iron and slag through a packed bed of coke particles in the dripping zone [20, 21, 22]. To

fulfill our ultimate goal, which is the modeling of a blast furnace using the XDEM, the phenomena inside the CZ also need to be modeled. Here, the main focus in this contribution is to model the softening process of iron-bearing materials in a pilot scale. Then, the results are analyzed regarding the gas and solid flow, temperature field, particle deformation, and pressure drop.

2. Model description

The XDEM method based on a Eulerian-Lagrangian framework is suitable for many engineering applications. A comprehensive description of the XDEM platform and its applications can be found in Peters et al. [23], however, the equations used in this contribution are explained here. In the XDEM platform, the solid particles are considered as discrete entities and the gas phase as a continuous phase that exchange momentum, heat, and mass between each other. In this section, the governing equations for the gas phase are described. Then, the equations to predict the position, orientation, and velocity along with temperature distribution of each particle individually are discussed. Later, the correlations used to calculate the coupling terms in the XDEM are presented. Finally, the XDEM dual-grid approach is recalled.

2.1. Fluid Phase Governing Equations

The governing equations consisting of mass, momentum and energy conservations for the gas phase are presented in Table 1. These equations are derived based on a Eulerian volumetric and time averaging method for porous media proposed by Faghri and Zhang [24]. The void space (ϵ) , also known as porosity, refers to the void spaces between the solid particles. The importance of this parameter in the porous media is undeniable and its accurate prediction is crucial particularly in the CZ. In the CZ, the iron ore particles are softened, which will lead to the creation of low void spaces and as a consequence, this phenomenon can change the gas phase passage locally. The XDEM void space calculation method was explained in our previous study [25]. The coupling parameters such as the fluid-particle interaction forces (\vec{F}_d) and the heat transfer coefficient (α) are described in the Table 4.

Table 1: The governing equations of the gas phase.		
Void space	$\epsilon = \frac{V_g}{V_{cell}} = 1 - \frac{V_s}{V_{cell}}$	
Conservation of mass	$\frac{\partial}{\partial t}(\epsilon \rho_g) + \nabla \cdot (\epsilon \rho_g \vec{v_g}) = 0$	
Conservation of momentum	$\frac{\partial}{\partial t}(\epsilon \rho_g \vec{v_g}) + \nabla \cdot (\epsilon \rho_g \vec{v_g} \vec{v_g}) =$	
	$-\epsilon \nabla p + \epsilon \rho_g g + \nabla \cdot [\epsilon \mu (\nabla \vec{v_g} + \nabla (\vec{v_g})^T)] + -\vec{F_d}$	
Conservation of energy	$\frac{\partial}{\partial t}(\epsilon \rho_g h_g) + \nabla.(\epsilon \rho_g \vec{v}_g h_g) =$	
	$-\nabla \cdot (\epsilon \lambda_g \nabla T_g) - \alpha (T_g - T_s)$	

2.2. Particles Governing Equations

The motion and position of each particle are predicted using a discrete element method based on the soft-sphere model, in which the particles are allowed to be overlapped in order to represent the softening behaviour of pellets. In this method, Newton's and Euler's second law for translation and

rotation of each particle, which are given in Table 2 are integrated over time. The contact force \vec{F}_i^c of a particle is described by the Hertz-Mindlin model [26, 27], which is a non-linear model for the contact force. The \vec{F}_i^c is the sum of all normal and tangential collision forces generated while colliding with the neighboring particles. This model was successfully employed by Baniasadi et al. [15] and Yang et al. [12, 13]. Based on this model, the contact force is non-linearly proportional to the overlap between particles and the mathematical model to calculate the contact force is also given in Table 2.

Table 2: The equations in the dynamic module of the XDEM platform.

Newton's second law of translation	$m_i \frac{d\vec{v_i}}{dt} = m_i \frac{d^2 \vec{x_i}}{dt^2} = \vec{F_i}^c + \vec{F_i}^g + \vec{F_i}^d$
Euler's second law of rotation	$I_i \frac{d\vec{\omega}_i}{dt} = \sum_{j=1}^n \vec{M}_{i,j}$
Normal contact force	$\vec{F}_{i,j}^{c,n} = -k_n \delta_n^{\frac{3}{2}} - c_n \delta_n^{\frac{1}{4}} \dot{\delta}_n$
Overlap	$\delta_n = r_i + r_j - \vec{x}_i - \vec{x}_j $
Normal spring stiffness	$k_n = -\frac{4}{3}E_{i,j}\sqrt{R_{i,j}}$
Normal viscous damping coefficient	$c_n = lne\sqrt{\frac{5m_{i,j}k_n}{\pi + lne^2}}$
Effective radius and reduced mass	$\xi_{i,j} = \frac{\xi_1 \xi_2}{\xi_1 + \xi_2}$, $\xi = R, m$
Effective Young's modulus	$\frac{1}{E_{i,j}} = \frac{1 - v_i^2}{E_i} + \frac{1 - v_j^2}{E_j}$
Tangential contact force	$\vec{F}_{i,j}^{c,t} = min[k_t \delta_t + c_t \dot{\delta}_t , \mu \vec{F}_{i,j}^{c,n}]$
Tangential stiffness	$k_t = -8G_{i,j}\sqrt{R_{i,j}\delta_n}$
Tangential dissipation coefficient	$c_t = lne\sqrt{\frac{5(4m_{i,j}k_t)}{6(\pi + lne^2)}}$
Effective shear modulus	$\frac{1}{G_{i,j}} = \frac{2 - v_i}{G_i} + \frac{2 - v_j}{G_j}$

The particle softening behaviour is closely related to the temperature.

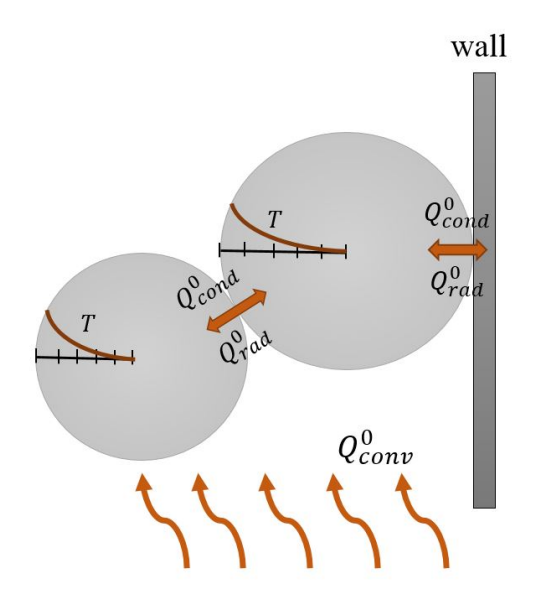


Figure 2: Illustration of heat exchanges between particles and wall.

Therefore, the key step to applying CFD-DEM to study the phenomenon in the CZ is that heat transfer must be considered. The XDEM has been already enhanced and validated for fluid-particle heat up process [18, 19, 28, 29, 30]. To investigate the softening process in high temperature, the heat exchange between particle-particle, and particle-gas along with the temperature gradient within the particle should be taken into account as illustrated schematically in Figure 2. The conversion module of the XDEM provides those by considering a system of one-dimensional and transient energy equation and the boundary conditions as written in Table 4. q'_{cond} and q'_{rad} account for conductive heat and radiation transport through physical contact with the wall and/or particles. $F_{P,j}$ is the view factor between the particle p and its neighbor j. For a more detailed derivation of the above equations the reader

is referred to Peters [17].

Table 3: The equations in the conversion module of the XDEM platform. Energy equation
$$\frac{\partial}{\partial t} \left(\rho h \right) = \frac{1}{r^n} \frac{\partial}{\partial r} \left(r^n \lambda \frac{\partial T}{\partial r} \right)$$
Boundary condition
$$\lambda \frac{\partial T}{\partial r}|_{r=0} = 0$$
$$\lambda \frac{\partial T}{\partial r}|_{r=R} = \alpha (T_{inf} - T_s) + q'_{cond} + q_{rad}$$
$$q'_{cond} = \frac{\frac{T_p - T_j}{\Delta x_{pj}}}{1/\lambda_p + 1/\lambda_j}$$
$$q'_{rad} = \sum_{j}^{M} F_{P,j} (T_P^4 - T_j^4)$$

2.3. Fluid-particle Heat and Momentum transfer Models

In order to calculate the convective heat transfer between a sphere and fluid flow, the classical Nu-relation, Ranz and Marshall [31] is used in this study. The other coupling term is the momentum interaction term, which is the drag force, \vec{F}_d , depends on the relative velocity of the solid particle and fluid and the effect of presence of neighbouring particles. The drag force coefficient, β , is calculated using modified Ergun correlation [32]. The Ergun equation is a popular equation in gas-solid flow studies to describe gas pressure drop through the packed bed of particles and has been also used for the softening process by Kurosawa et al.[10]. The models are described in Table 4.

2.4. Dual-grid multiscale CFD-DEM coupling

In a dual-grid multiscale CFD-DEM coupling as introduced in [16], two length-scales are identified within the particle-laden flow. Fluid-particle in-

Table 4: The coupling model of the XDEM platform. Heat transfer coefficient $\alpha = \frac{Nu\lambda}{2r_p}$ Ranz-Marshall correlation [31] $Nu = 2 + 0.6Pr^{\frac{1}{3}}Re^{\frac{1}{2}}$ Drag force $\vec{F}_d = \frac{\beta V_p}{(1-\epsilon)}(v_g - v_p)$

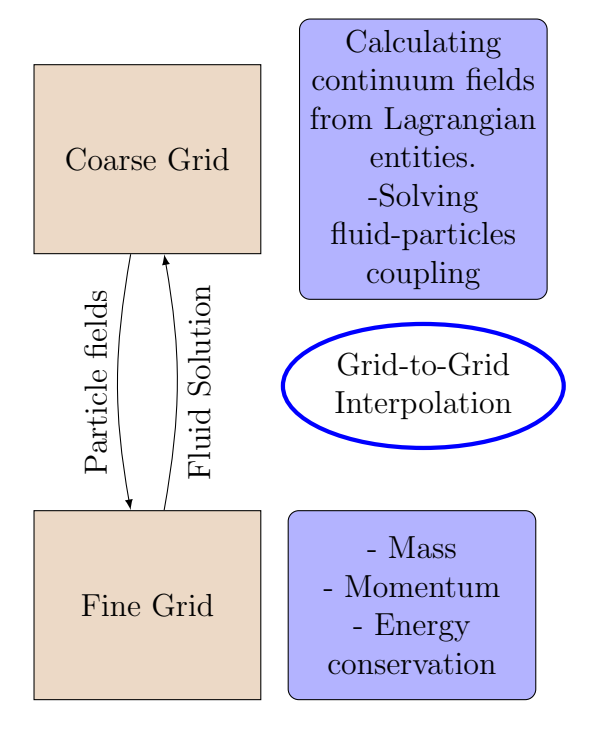


Figure 3: Diagram of the solution procedure within a dual-grid multiscale approach. The two boxes on the left represent the grids associated the bulk and the fluid-fine scale, while the arrows show schematically the communication between the scales. The coarse grid (top) is used to map the Lagrangian field of the DEM into an Eulerian reference and to solve the fluid-particle interaction. Particle-related fields are mapped to the supporting domain (bottom) where a finer grid is used to solve the fluid equations.

teractions are resolved on a bulk scale that is the one typically used for CFD-DEM couplings based on the volume averaging technique. The main assumption on this lengthscale consist in considering particles as zero-dimensional entities interacting with the fluid with local exchanges of mass, momentum and energy. In order to enforce this hypothesis, a coarse and uniform grid is the most approapriate choice. The fluid equations are discretized on fluid fine-scale that is different from the previous one and chosen as the scale at which grid-convergent results can be ensured. For this, fine grid discretizations are normally required, particularly for configurations featuring high-velocity flows and complex multiphase phenomena [16].

As shown in Figure 3, a coarse and uniform grid is adopted to resolve the bulk scale, namely the calculation of the void space field, drag, and heat source according to what presented in sections 2.1 and 2.3. A fine grid is instead used to solve the fluid flow equations at the fine-scale, namely the conservation of mass, momentum and energy as proposed in section 2.1. An interpolation strategy ensures the communication between the two grids i.e. the two lengthscales. As originally done in [16], the interpolation between meshes is performed via the *OpenFOAM-extend meshToMesh* library.

This multiscale approach to CFD-DEM couplings was originally proposed in [16, 33] and was successfully applied to study different complex flow configurations [34, 35]. In this contribution, the dual-grid multiscale approach is chosen in order to obtain grid-independent solution for the gas phase flow within the BF. As shown in 3.1.2, grid-independent solutions are only obtained with discretization finer than the single-scale one.

3. Results and Discussion

In this work, the modelling of the softening process of pre-reduced iron ore pellets in the CZ is intended. Pellets are one of the primary feed sources for blast furnaces. It is believed that pellets are reduced by the reducing gas in the shaft, above the CZ, to a Reduction Degree (RD) more than 50% and less than 80% [36, 37]. The RD is defined as the ratio of the oxygen removal and the total mass of removable oxygen initially present in the iron ore. Then, they are softened and molten and generating two different liquids: molten iron and primary slag. The behaviour of the partially reduced pellets during the softening process might depend on several variables. The pellets start deforming at a temperature that depends on the type of sample, the reduction degree (RD) and the load [38]. Nonetheless, Baniasadi et al. [15], Nogueira et al. [39], and Kemppainen et al. [40] proved that the RD has not a significant effect on the softening of the reduced pellets to RDs between 50-80%. Moreover, the best estimate for the load, the weight of the burden above the CZ, is 100kPa [36, 37]. Therefore, the type of the pellet and its composition are the main factors in the softening process. In this study, we selected a type of pellets which is an acid pellet from a working plant. The composition of the pellet is shown in Table 5. It is assumed that the pellets are partially reduced to the RD of 70%. The composition of the reduced pellet is obtained according to the iron oxide reduction reactions [18, 19] by using a simple mass balance calculation as shown in Table 6. It is assumed the slag consists of FeO, SiO_2 , CaO, MgO, and Al_2O_3 .

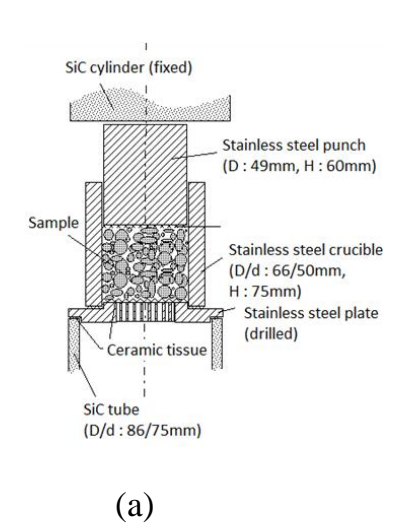
To model the softening process of pellets in a real BF, the XDEM should be first validated for this process. For this reason, the softening experiments for a lab-scale packed bed of reduced pellet were carried out. A small crucible filled by the pellet particles as illustrated in Figure 4 (a) was placed inside a big furnace. A stainless steel punch was used to exert 100KPa load on the top of particles. The temperature of the furnace is increased gradually from 800 to $1100^{\circ}C$, and the hight changes of the bed of particles are recorded over temperature. The process was simulated by the XDEM and the results for the evaluation of the bed shrinkage over temperature was compared with the experimental results as shown in Figure 4 (b). Consequently, an appropriate relationship between Young's modulus and temperature for the studied pellets has been established. For more details of the experiments and simulation results, the reader is referred to [15]. In this study, the main target is to apply the validated model for describing the softening process in a larger scale close to a real BF condition.

Table 5: Chemical composition of the iron ore pellet.

Component	$\mathrm{Wt}(\%)$
Fe_2O_3	92.43
FeO	0.57
SiO_2	4.22
CaO	1.42
MgO	0.55
Al_2O_3	0.39
inerts	rest

Table 6: Chemical composition of the reduced iron ore pellet.

Component	Wt(%)
Fe	56.1
Slag	43.9



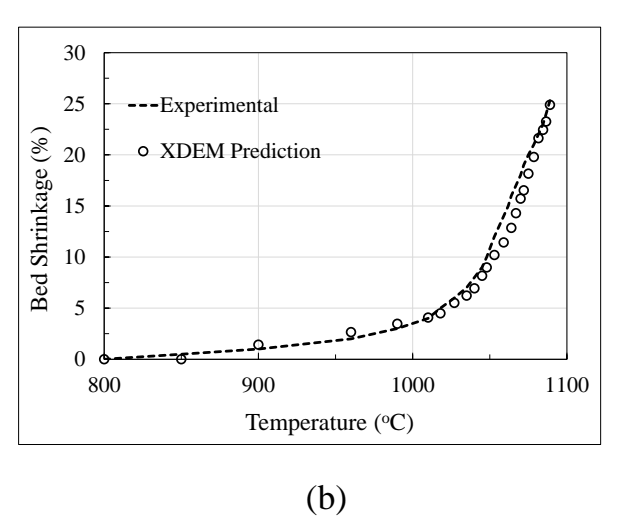


Figure 4: (a) The experimental setup. (b) Comparison of the XDEM results and experimental data for the bed shrinkage.

3.1. Simulation results

3.1.1. The simulation setup

To verify the gas-solid interaction during the softening process of the iron ore pellets in a larger scale, the bottom part of the LKAB's Experimental Blast Furnace (EBF) [41, 42] is considered. LKAB's EBF was built primarily for product development of iron ore pellets in 1999. It is used for the evaluation of the burden materials as well as the investigation of new blast furnace operational concepts and equipments [43]. The EBF has a working

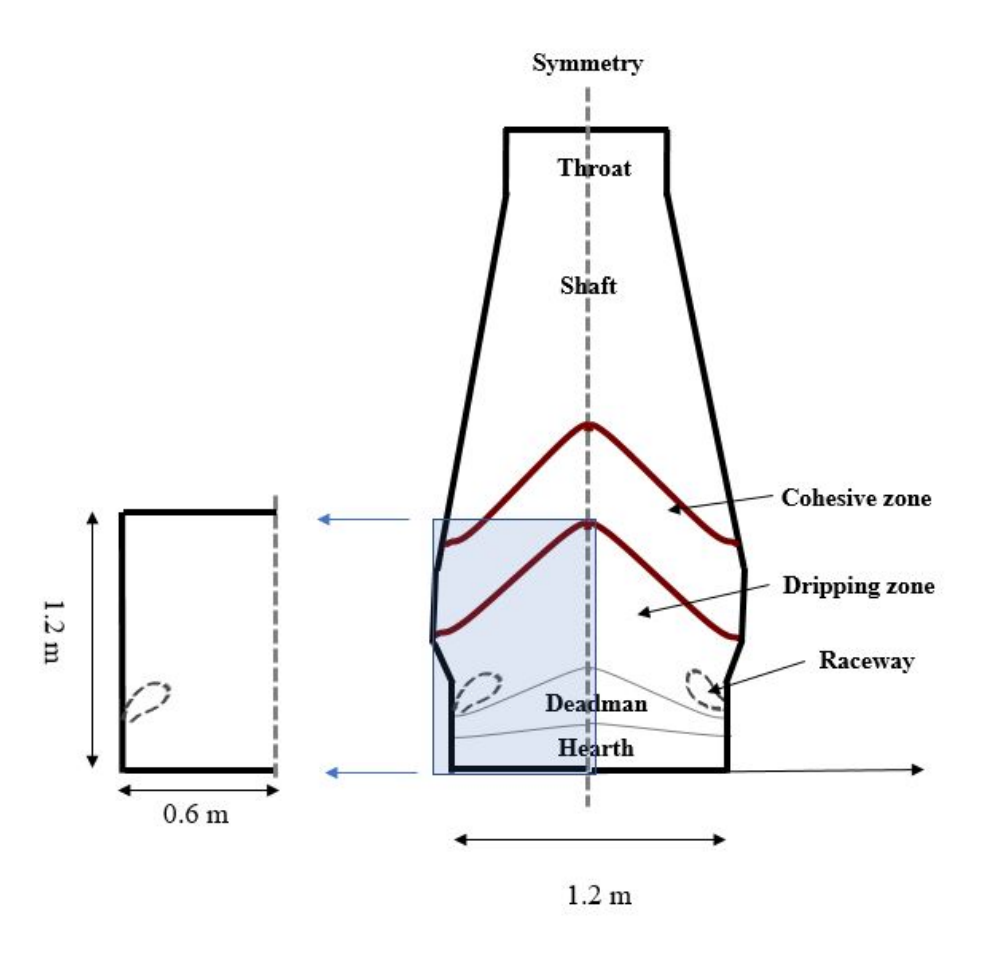


Figure 5: Schematic diagram of different parts of the LKAB's EBF and the zone defined to investigate the gas-solid interaction during the softening process.

volume of $8.2m^3$ with the diameter of 1.2m at tuyere level. The operation of the EBF is similar to a commercial blast furnace, although with a smaller size. A two-dimensional schematic of the EBF is shown in the right hand side of Figure 5. The part of the EBF considered in our simulation is illustrated in the left hand side of Figure 5, while neglecting the radial variations. To reduce the computational time, a symmetric 2D model is considered which is often used in the BF modelling [44, 45, 46]. This section was provided for the simulation with the alternating layers of ore and coke above the CZ and only stationary cokes below that. This can be performed by the dynamic module of the XDEM, which tracks the motion of each particle under gravity and its dynamic collisions with other particles and boundaries. Figure 6 represents the setup used in this simulation. The coke and pellet are coloured by their sizes. The pellets' size range form 11mm to 13mm and the cokes 19 to 21mm [41]. Cokes in front of the tuyere are assumed being consumed by combustion thus creating voidage. The shape of the CZ is dependent on the burden distribution. Two basic types of the CZ can be discriminated: inverted V and W [47]. In this study, inverted V shape is assumed for the CZ. In this type, the center of the furnace only contains coke. Therefore, in the center of the furnace, no softening and melting would occur.

3.1.2. Gas-solid interaction characterization

The generated setup is provided by specifying an inlet gas at a temperature of 2500K and at a velocity of 150m/s. The initial temperature for

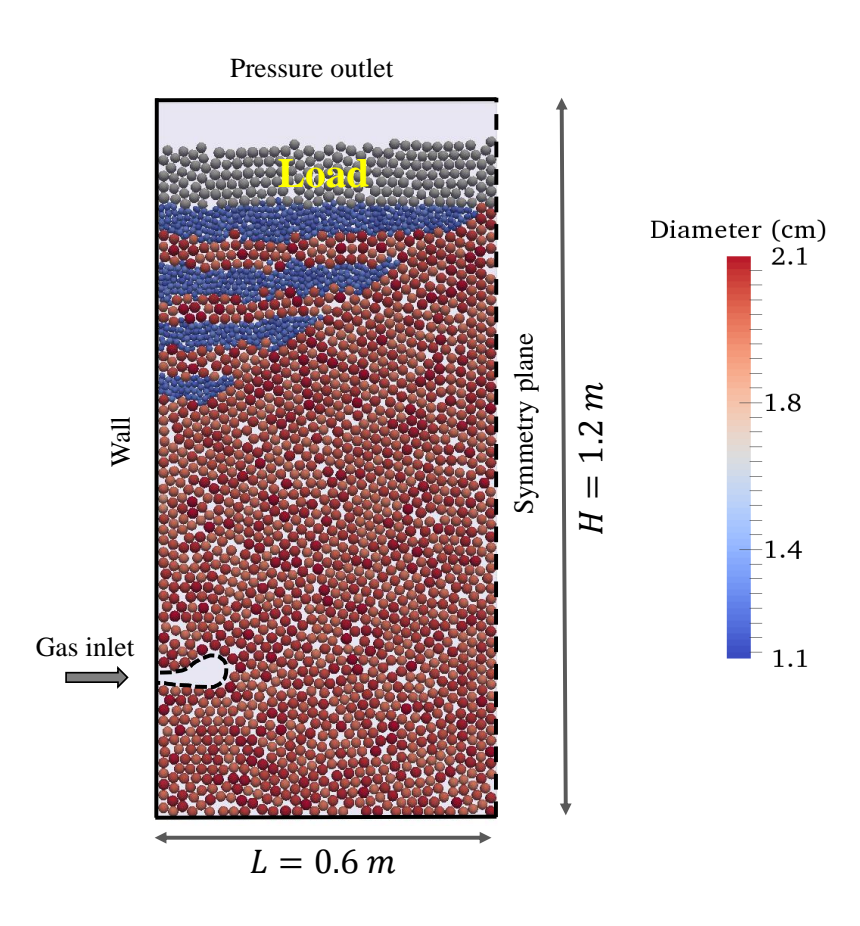


Figure 6: The model geometry filled with the alternating layers of ore and coke above the CZ and only coke below that. The top layer acts as a load representing the weight of burden above the CZ.

the coke and pellet particles and the gas is considered to be 1250K because below that the softening of the pellets is negligible according to the results of the small-scale softening experiments [15]. Table 7 shows the required parameters used in the simulation. The simulation time was 40 seconds when the temperature of pellets in the upper layer reaches to 1377K, which is the melt onset temperature of the studied pellet estimated in the previous study [15]. The time is shown as a dimensionless form as t^* . It should be noted that, the liquid phases are not considered in this study.

The velocity of the injected gas from tuyeres of the LKAB's EBF is high. Thus, the appropriate reconstruction of fluid dynamics requires refining the CFD grid. Moreover, the calculation accuracy of gas velocity and the temperature is substantial. These variables influence the convective heat transfer between particle and gas which is responsible for the heat up, reduction and melting of particles. Therefore, it may change the softening and melting behaviour of iron-bearing materials and as a result, the BF productivity. To achieve this high level of accuracy, the scheme explained in section 2.4 is used. To find the best CFD construction, the grid independence of the solution was studied on the gas velocity at the tuyere level as shown in Figure 7. The number of cells was varied in the range of 2046–73656. An underestimation of the gas velocity in the cases with coarser meshes is observed. The simulation was found to be grid independent when the number of cells exceeded 32736 where no significant changes were observed by refining the mesh. Therefore, the grid system having 16 times cells more than the coarse

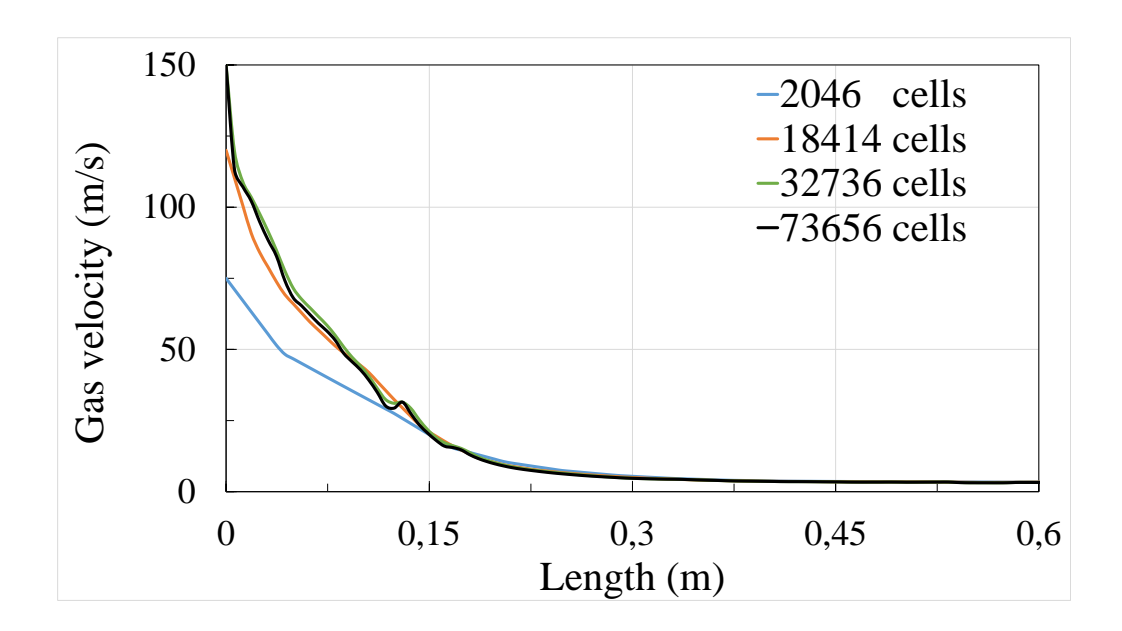


Figure 7: The gas velocity magnitude for four different cell numbers over the length at height of 0.25m (tuyere level) and $t^* = 1$.

mesh was used to resolve the details of flow, and temperature fields. The model geometry with coarse and fine meshes is represented in Figure 8.

The most significant phenomena experienced by the softening are the heat transfer and the gradient changes of permeability, pressure drop and gas flow path, which can be attributed to the deformation of particles. Therefore, temperature and micro-dynamics of particles like displacement and deformation cause voidage reduction, thus affect the gas flow field, and pressure drop. These phenomena are used to demonstrate the general features of the soften-

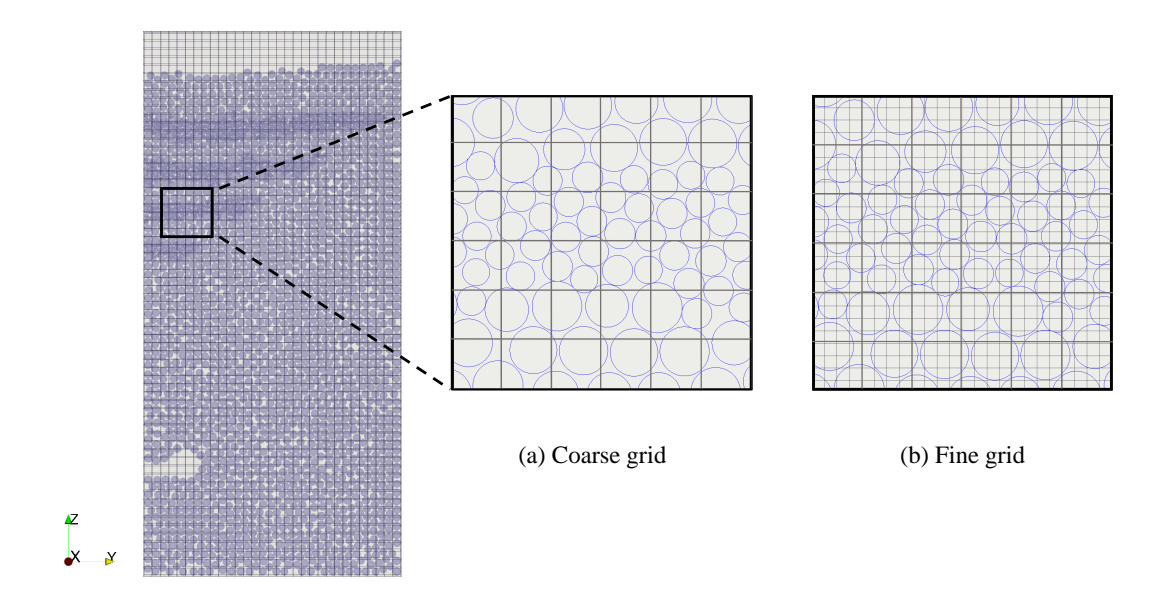


Figure 8: Representation of the number of cells in the (a) coarse grid with 2046 cells and (b) fine grid with 32736 cells.

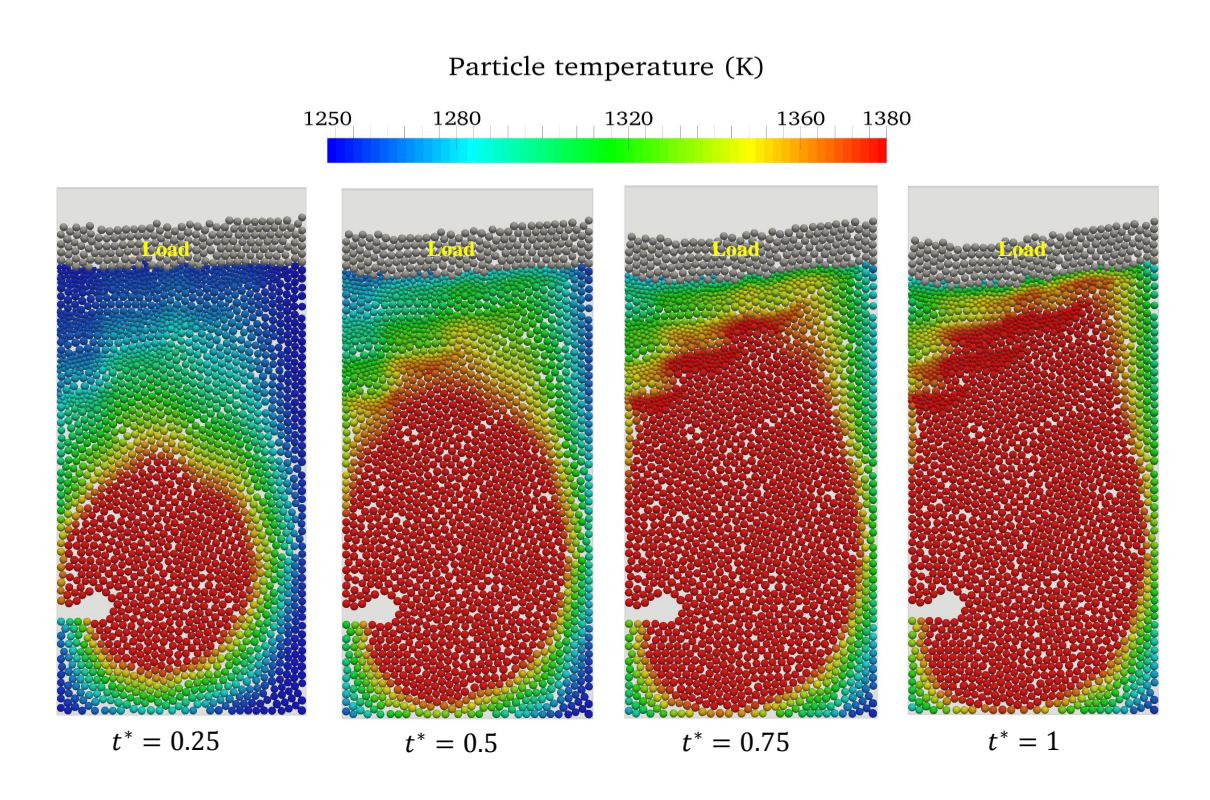


Figure 9: Particle temperature evaluation over time.

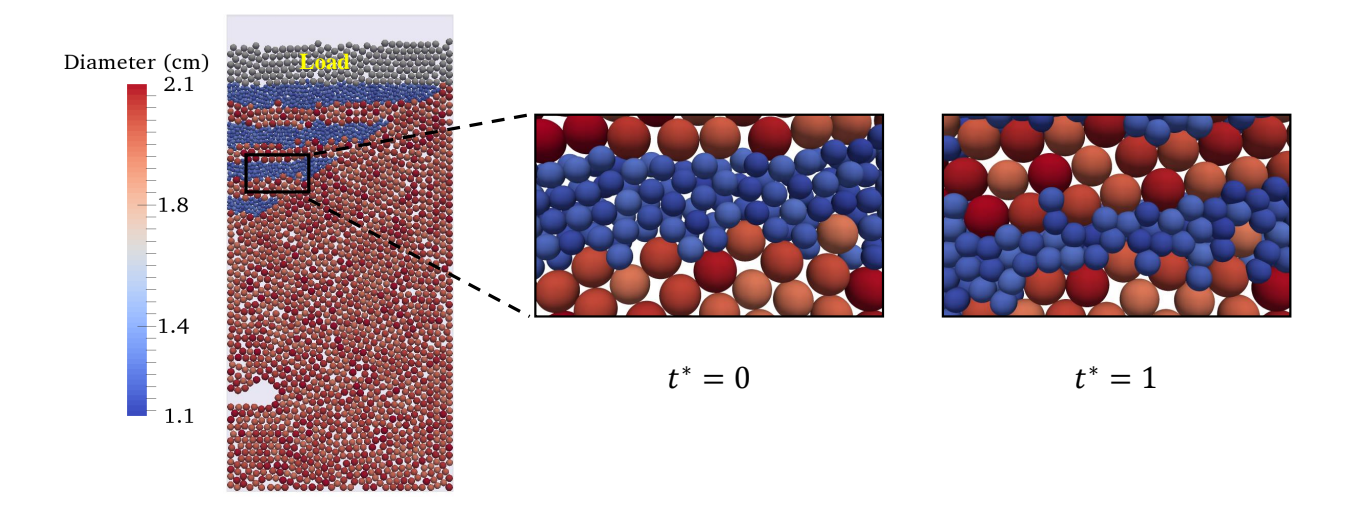


Figure 10: Initial and final structure of a layer of coke and pellet in a closer view.

ing process. To describe them accurately, a validated and verified approach for particle heating up by a hot fluid, and the rheology of gas facing particles is needed. The XDEM which is a CFD-DEM method coupled with the heat transfer has been validated for the heat transfer in packed beds including convective, particle-particle conduction, and particle radiation [15, 18, 19]. Besides, the pressure drop of a gas flow in a packed bed for different particle sizes was appropriately described by Baniasadi and Peters [21]. Therefore, the XDEM is a reliable tool to be applied to the softening process.

The particles are heated up by absorbing convective heat from the hot gas passing through the void spaces. As the pellets are heated up, they start softening over the temperature due to the decrease of Young's modu-

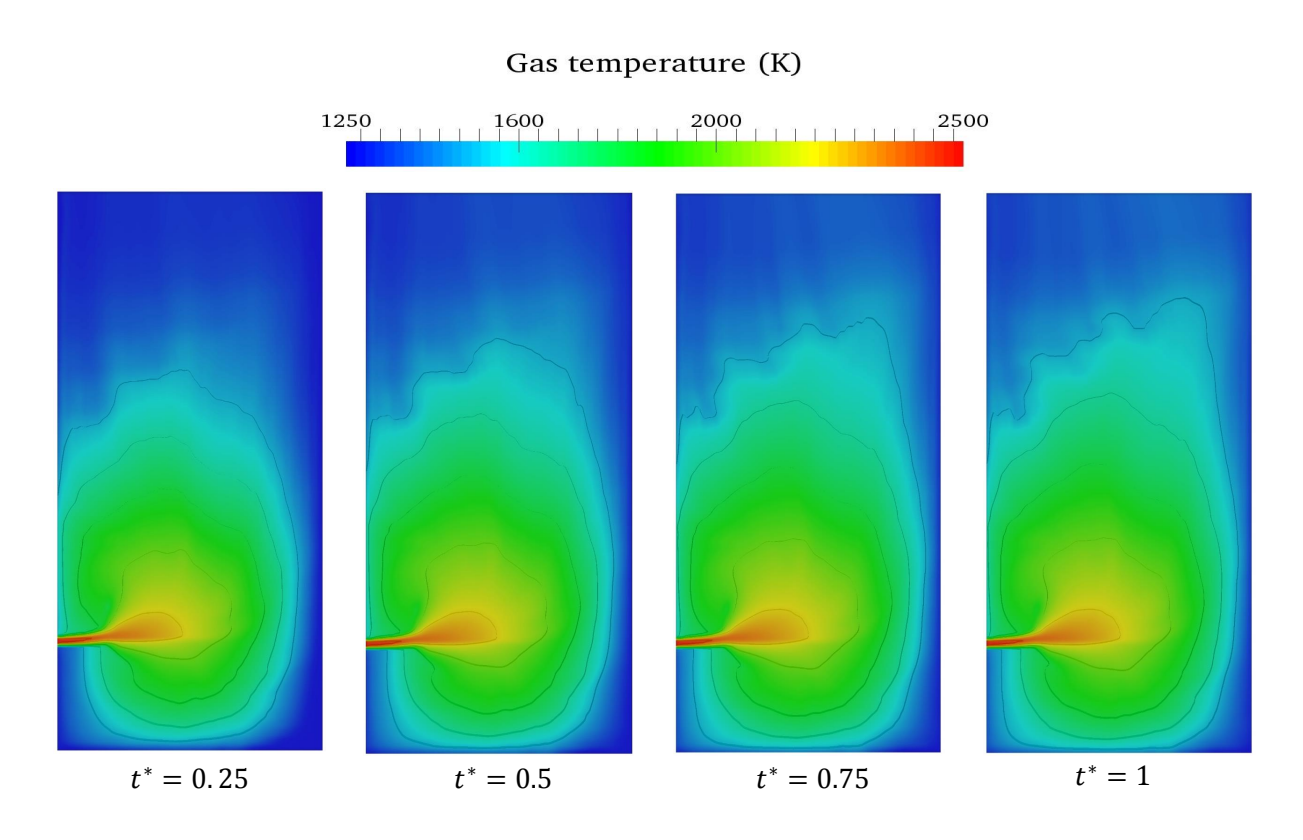


Figure 11: Gas temperature evaluation over time.

Table 7: Thermal and mechanical properties of the reduced pellet and coke used in the XDEM simulation.

Property	Pellet	Coke
Thermal conductivity $(Wm^{-1}K^{-1})$	0.5 [48]	0.96 + 0.00183 * T [49]
Heat capacity $(Jkg^{-1}K^{-1})$	1000 [48]	320 + 0.61 * T [49]
Intrinsic density (kgm^{-3})	3000	1000
Coulomb friction coefficient	0.7 [50]	0.9[51]
Restitution factor	0.15[52]	0.2[51]
Poisson ratio	0.24 [52]	0.3 [51]

lus. Naturally, the lower pellet layer softens first due to facing the gas inlet earlier. The height of the moving bed decreases more remarkably with further softening in the upper layers. Figure 9 shows the evaluation of particles temperature for different instances. It can be seen that the structural changes in the packed bed when the temperature increases and the position of the particles vary with time because the layers of pellets undergo shrinkage by particles' overlapping. This phenomenon is presented in Figure 10 for a part of a layer in a closed view. It can be seen that the structure of the ore layer changes significantly from initial state $(t^* = 0)$ to the final state $(t^* = 1)$, however, the coke particles are not softened and remain intact due to their mechanical strength. Additionally, the thermal energy of the gas is reduced as it travels through the packed bed due to the cooling effect of the particles. Thus, further upstream the gas temperature is reduced. On the other hand, as the bottom cokes and lower pellet layer are heated up and the temperature difference between them and the gas phase decreases, the hot gas can supply more thermal energy for the upper layers. The evaluation of the gas temperature with iso-surfaces is shown in Figure 11. One can observe how the heat absorption of coke and pellet induces changes in the gas temperature distribution, allowing clear identification of the cohesive zone by simply looking at the iso-temperature contours.

As observed, the softening changes the local structures of the moving bed, void space between particles, and hence the gas flow. The initial void space distribution of the model geometry calculated by the XDEM is shown in Figure 12. It is nearly 0.4 for the iron ore pellets layers, 0.55 for the coke layers, and 1 in where no particles exist such as the raceway. To see the changes during the softening process in a better visualization, the evolution of void space and the gas flow is shown in Figure 13 for the marked region of Figure 12, in where ore layers exist. The void space is displayed in a contour plot, with vectors showing the gas velocity field. It can be seen that, at the beginning, gas flows evenly upwards. When the softening process begins, the overlap of pellet particles evolves, and subsequently, the void space of the pellet layers reduces and eventually reaches almost 0.2. To better observe the phenomenon, the point A is selected and the local porosity changes over time for that point is presented in Figure 14. In this figure, it is possible to observe how the shrinking process starts at $t^* = 0.2$, and up to $t^* = 1$ the void space decreased to almost half of its initial value. It is also possible to observe how the process is faster between $t^* = 0.4$ and $t^* = 0.8$ when the derivative of the void space over time is clearly changing. This phenomenon was already observed, under simpler conditions, in Figure 4, and confirms

once more the non-linear nature of the bed-shrinkage.

The reduction of the void space affects the gas flow significantly in both magnitude and direction. In particular, as shown in Figure 13, the gas flow loses its uniformity. The velocity vectors can be observed to bend in the proximity of the low-porosity zones and find alternative paths toward higher porosity regions. Figure 15 shows the evaluation of the gas velocity over time at the center of the bed for the point B. It is interesting to observe how the velocity magnitude in point B is clearly correlated to the porosity changes shown in Figure 13. In particular, the rise in velocity starts around $t^* = 0.2$, and reaches almost 1.5 times its original value at $t^* = 1$. This underlines the importance of the mutual interaction between the gas flow and the particles dynamics and therefore the significance of a numerical method able to resolve them together. In order to track the gas flow pattern in the whole domain from the entrance to the top, the stream lines of the gas flow colored by their magnitude are presented in Figure 16. It should be noted that the gas flow is not the only hydrodynamic parameter affected by the softening process. This phenomenon has also a profound effect on the pressure drop. This basic fluid-dynamic relation is here particularly delicate. As a matter of fact the pressure drop in static conditions is known to be a function of both porosity and velocity. Due to the fact that within the CZ of the BF the porosity changes dynamically, and, as a consequence, it changes dynamically the gas velocity, pressure drop predictions based on static conditions are no longer accurate. This is a further motivation to apply CFD-DEM models to study the BF process, as the extremely important operative parameter of the pressure drop is very difficult to be predicted else way. In Figure 17 the obtained pressure drop over the height of the specified zone is depicted. As can be seen, the pressure drop increased over time due to the development of the softening process. The pressure drop is enhanced with a sharper slope due to the low value of void space when the particle's temperatures are close to the melting point.

As it observed the proposed approach has the possibility of monitoring global features of the flow with local parameters in the CZ, and opens the path for the possible future developments to study the CZ of the BF in a real condition.

4. Conclusions

The eXtended Discrete Element Method (XDEM) has been applied to describe the softening behavior of pellets in the cohesive zone of an experimental blast furnace. The XDEM is a CFD-DEM method coupled with heat transfer between gas-particle and particle-particle conduction and radiation that are significant for the softening process as well as for all processes taking place in the BF. The XDEM is also enhanced with dual-grid multiscale approach coupling which is a necessity when the fluid velocity is high, in particular, in the raceway of a blast furnace. In conclusion, the developed model is verified for gas-solid behaviour during the softening process, in which the deformation of particles is expressed by the overlapping approach. In this

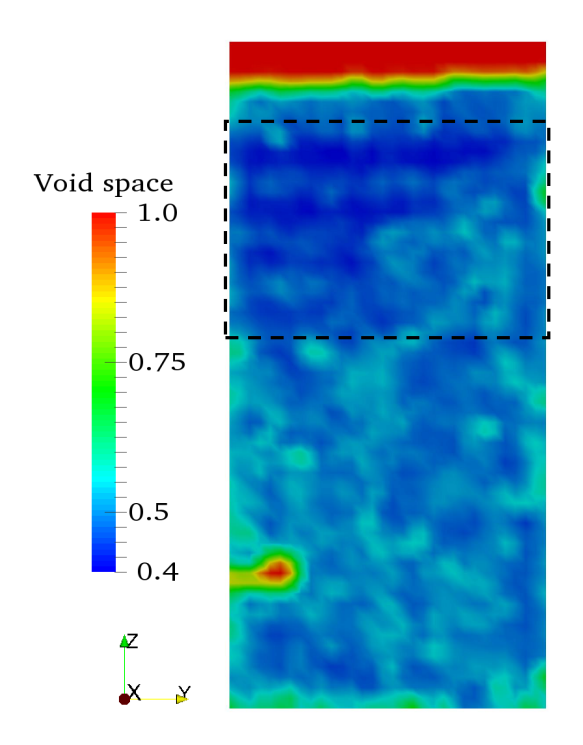


Figure 12: Void space distribution of the model geometry calculated by the XDEM.

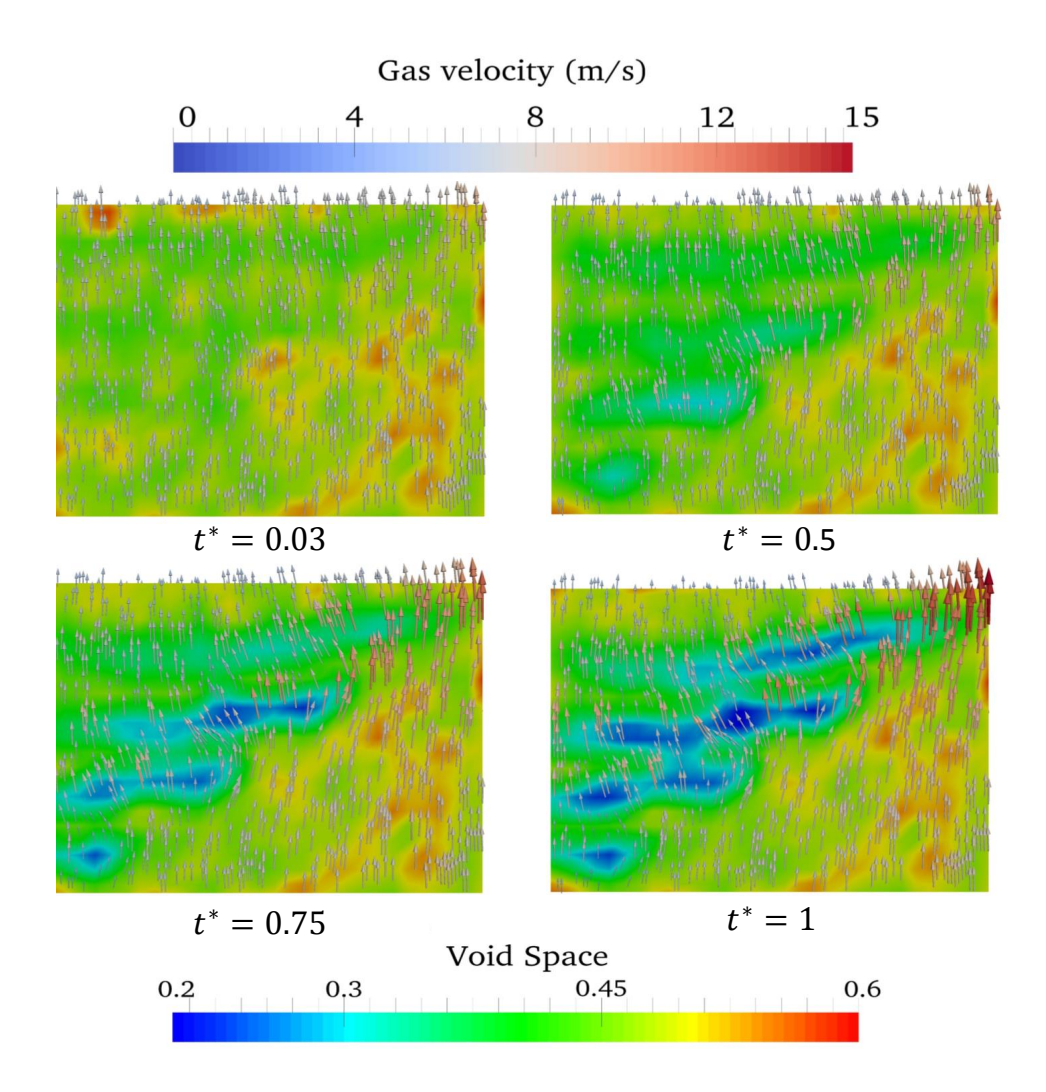


Figure 13: Gas vectors and void space evolution over time on the zone shown in Figure 12.

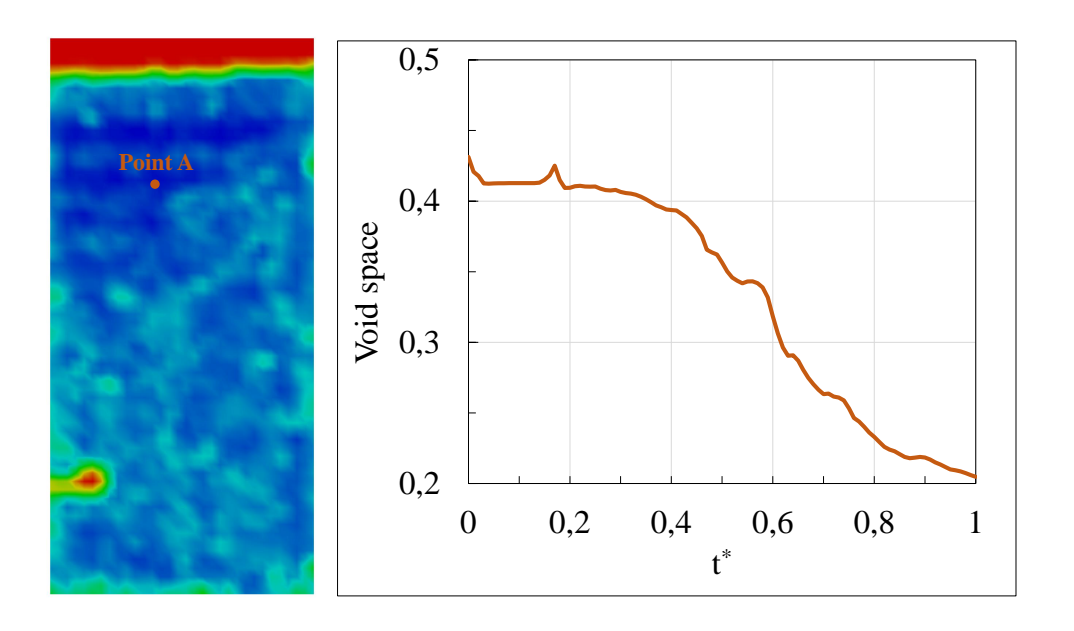


Figure 14: The local changes of the void space over time in the point A.

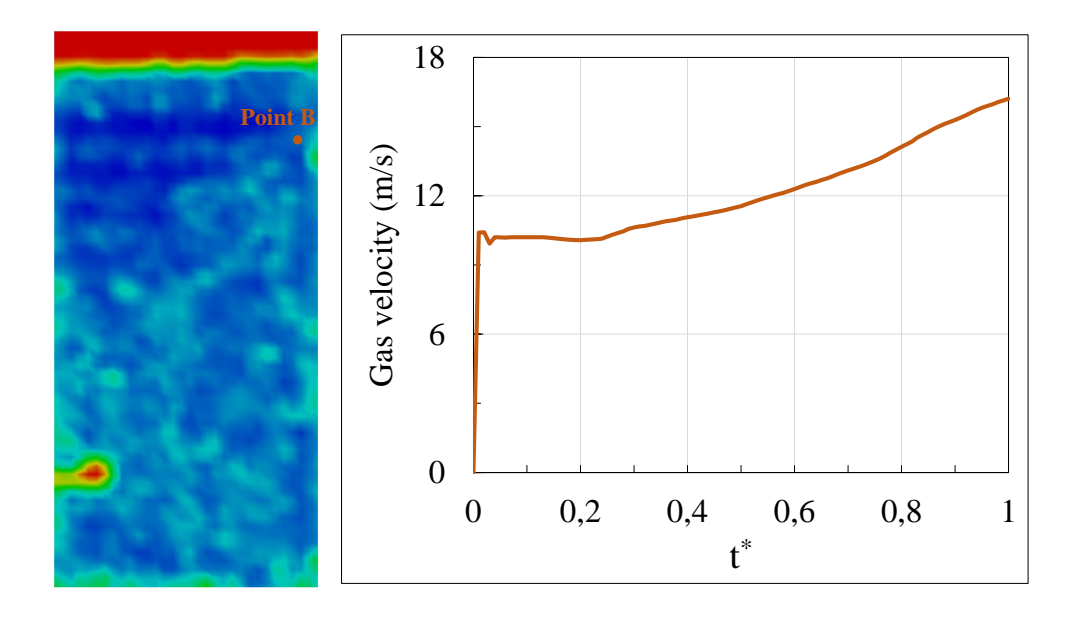


Figure 15: The local changes of the gas velocity over time in the point B.

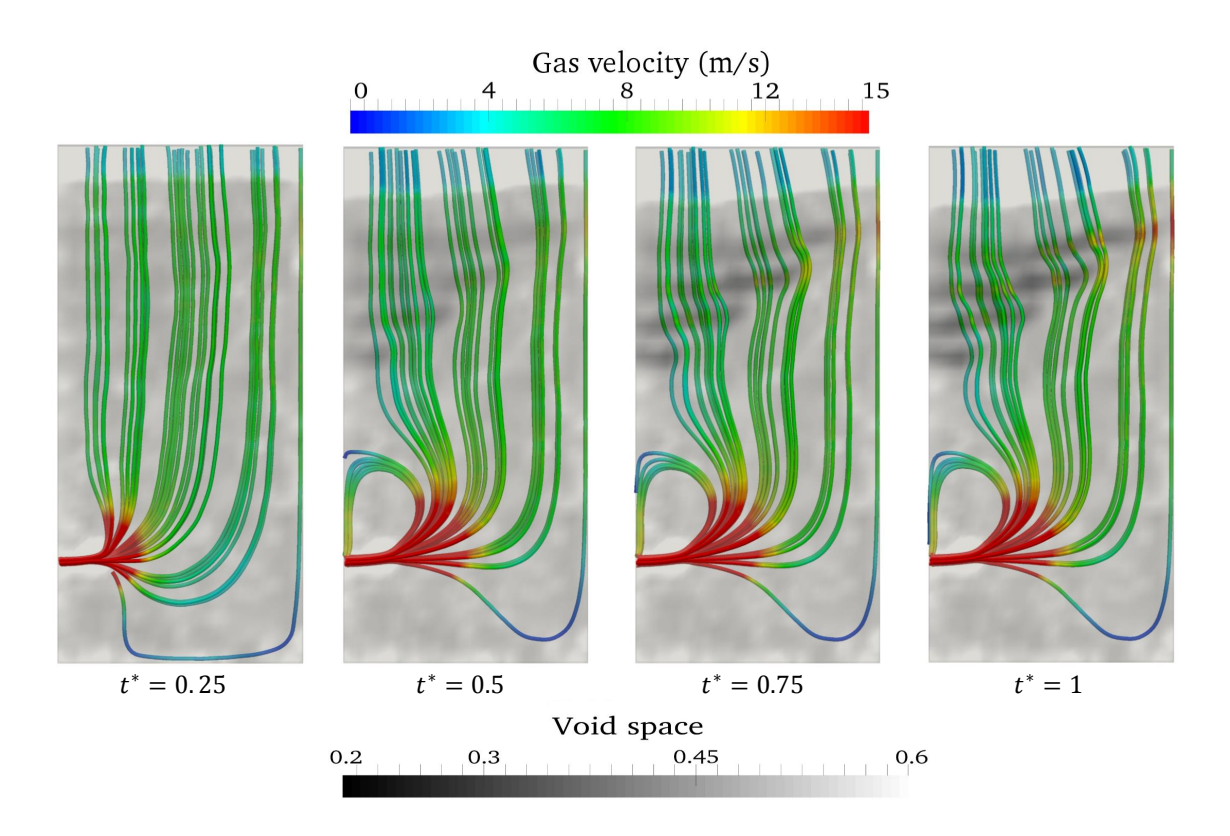


Figure 16: Gas stream lines over time.

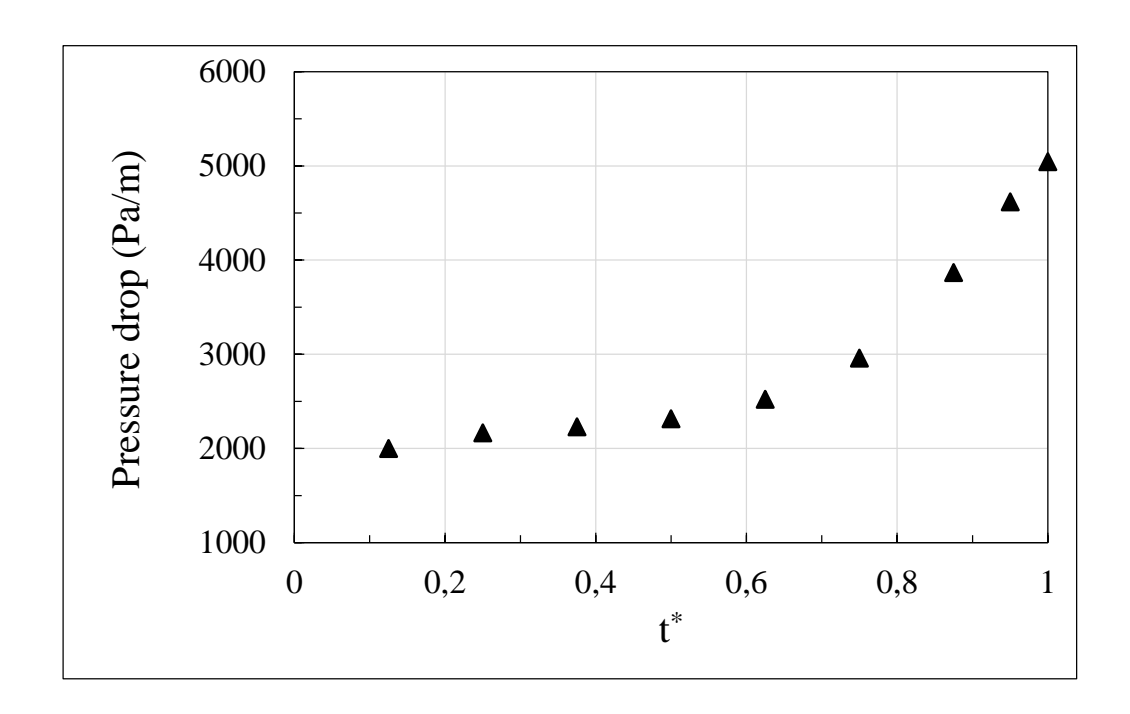


Figure 17: Pressure drop changes over time on the zone shown in Figure 12.

study, the parameters such as the deformation, displacement, and temperature of the particles on the one hand and the gas phase temperature, velocity, and pressure drop, on the other hand, were analyzed. In the end, the mutual effects of the gas and solids were comprehensively studied. Although, any reactions and melting process were not considered, it was observed that the findings are useful to establish a model for identification of a cohesive zone of a blast furnace in the real condition.

Acknowledgements

The authors are thankful to the Luxembourg National Research Fund (FNR) and the HPC group of the University of Luxembourg.

```
Nomenclature
       gravitational accelerating (ms^{-2})
g
t
       time (s)
T
       temperature (K)
       enthalpy (Jkg^{-1})
h
       particle radius (m)
r
       particle mass (kg)
m
       position (m)
x
       heat flux (Wm^{-2})
q'
       velocity (ms^{-1})
v
V
       volume (m^3)
p
       pressure (Pa)
F
       force (N)
       momentum of inertia (jkg^{-1})
Ι
M
       torque (Nm)
Greek Symbols
       void space (-)
\epsilon
       heat transfer coefficient (Wm^{-2}K^{-1})
\alpha
       thermal conductivity (Wm^{-1}K^{-1})
λ
       density (kqm^{-3})
ρ
       dynamic viscosity (kgm^{-1}s^{-1})
\mu
\delta
       overlap (m)
       angular velocity (rads^{-1})
Superscripts and Subscripts
       particle
i, j
       particle
p
       contact forces
c
       normal direction
n
       tangential direction
t
rad
       radiation
cond
       conduction
       ambient
inf
       dimensionless
```

gas

solid

drag

g

 $\frac{s}{d}$

References

References

- [1] M. Baniasadi, Resolving multiphase flow of trickle bed reactors by the extended discrete element method (xdem) applied to the blast furnace, Ph.D. thesis, University of Luxembourg (2018).
- [2] A. Babich, D. Senk, Ironmaking, RWTH Aachen University, 2008.
- [3] J. Yagi, Mathematical modeling of the flow of four fluids in a packed bed, ISIJ International 33 (6) (1993) 619–639. doi:10.2355/isijinternational.33.619.
- [4] P. R. Austin, H. Nogami, J. ichiro Yagi, A mathematical model for blast furnace reaction analysis based on the four fluid model, ISIJ International 37 (8) (1997) 748–755. doi:10.2355/isijinternational.37.748.
- [5] P. R. Austin, H. Nogami, J. ichiro Yagi, A mathematical model of four phase motion and heat transfer in the blast furnace, ISIJ International 37 (5) (1997) 458–467. doi:10.2355/isijinternational.37.458.
- [6] Z. Miao, Z. Zhou, A. Yu, Y. Shen, Cfd-dem simulation of raceway formation in an ironmaking blast furnace, Powder Technology 314 (Supplement C) (2017) 542 549, special Issue on Simulation and Modelling of Particulate Systems. doi:https://doi.org/10.1016/j.powtec.2016.11.039.

- [7] Q. Hou, D. E, S. Kuang, Z. Li, A. Yu, Dem-based virtual experimental blast furnace: A quasi-steady state model, Powder Technology 314 (2017) 557 566, special Issue on Simulation and Modelling of Particulate Systems. doi:https://doi.org/10.1016/j.powtec.2016.12.017.
- [8] Y. Yu, H. Saxn, Segregation behavior of particles in a top hopper of a blast furnace, Powder Technology 262 (Supplement C) (2014) 233 – 241. doi:https://doi.org/10.1016/j.powtec.2014.04.010.
- [9] S. Ueda, T. Kon, H. Kurosawa, S. Natsui, T. Ariyama, H. Nogami, Influence of shape of cohesive zone on gas flow and permeability in the blast furnace analyzed by dem-cfd model, ISIJ International 55 (6) (2015) 1232–1236. doi:10.2355/isijinternational.55.1232.
- [10] H. Kurosawa, S. Matsuhashi, S. Natsui, T. Kon, S. Ueda, R. Inoue, T. Ariyama, Dem-cfd model considering softening behavior of ore particles in cohesive zone and gas flow analysis at low coke rate in blast furnace, ISIJ International 52 (6) (2012) 1010–1017. doi:10.2355/isijinternational.52.1010.
- [11] W. Yang, Z. Zhou, A. Yu, Discrete particle simulation of solid flow in a three-dimensional blast furnace sector model, Chemical Engineering Journal 278 (2015) 339 352, tailoring Sustainability through Chemical Reaction Engineering. doi:https://doi.org/10.1016/j.cej.2014.11.144.
- [12] W. Yang, Z. Zhou, D. Pinson, A. Yu, A new approach for studying

- softening and melting behavior of particles in a blast furnace cohesive zone, Metallurgical and Materials Transactions B 46 (2) (2015) 977–992. doi:10.1007/s11663-014-0223-8.
- [13] W. Yang, Z. Zhou, A. Yu, D. Pinson, Particle scale simulation of soft-eningmelting behaviour of multiple layers of particles in a blast furnace cohesive zone, Powder Technology 279 (Supplement C) (2015) 134 145. doi:https://doi.org/10.1016/j.powtec.2015.04.002.
- [14] S. J. Chew, P. Zulli, D. Maldonado, A. Yu, Melt down behaviour of a fused layer in the blast furnace cohesive zone, ISIJ International 43 (3) (2003) 304–313. doi:10.2355/isijinternational.43.304.
- [15] M. Baniasadi, B. Peters, J.-C. Pierret, B. Vanderheyden, O. Ansseau, Experimental and numerical investigation into the softening behavior of a packed bed of iron ore pellets, Powder Technology.
- [16] G. Pozzetti, B. Peters, A multiscale dem-vof method for the simulation of three-phase flows, International Journal of Multiphase Flow 99 (2018) 186 – 204. doi:https://doi.org/10.1016/j.ijmultiphaseflow.2017.10.008.
- [17] B. Peters, Thermal Conversion of Solid Fuels, WIT Press, 2003.
- [18] B. Peters, F. Hoffmann, D. Senk, A. Babich, Experimental and numerical investigation into iron ore reduction in packed beds, Chemical Engineering Science 140 (2016) 189 – 200. doi:http://dx.doi.org/10.1016/j.ces.2015.09.017.

- [19] B. Peters, F. Hoffmann, Iron ore reduction predicted by a discrete approach, Chemical Engineering Journal 304 (Supplement C) (2016) 692
 702. doi:https://doi.org/10.1016/j.cej.2016.06.116.
- [20] M. Baniasadi, B. Peters, Preliminary investigation on the capability of extended discrete element method for treating the dripping zone of a blast furnace, ISIJ International 58 (1) (2018) 25 – 34.
- [21] M. Baniasadi, B. Peters, Resolving multiphase flow through packed bed of solid particles using extended discrete element method with porosity calculation, Industrial & Engineering Chemistry Research 56 (41) (2017) 11996–12008. doi:10.1021/acs.iecr.7b02903.
- [22] M. Baniasadi, B. Peters, M. BaniasadiBaniasadi, X. Besseron, Hydrodynamic analysis of gas-liquid-liquid-solid reactors using the xdem numerical approach, The Canadian Journal of Chemical Engineering 0 (0). arXiv:https://onlinelibrary.wiley.com/doi/pdf/10.1002/cjce.23191, doi:10.1002/cjce.23191.
- [23] B. Peters, M. Baniasadi, M. Baniasadi, X. Besseron, A. E. Donoso, M. Mohseni, G. Pozzetti, The xdem multi-physics and multi-scale simulation technology: Review on dem-cfd coupling, methodology and engineering applications, Particulogy.
- [24] A. Faghri, Y. Zhang, Transport phenomena in multiphase systems, Academic Press, 2006.

- [25] M. Baniasadi, M. Baniasadi, B. Peters, Coupled cfd-dem with heat and mass transfer to investigate the melting of a granular packed bed, Chemical Engineering Science 178 (2018) 136 – 145. doi:https://doi.org/10.1016/j.ces.2017.12.044.
- [26] H. Hertz, Ueber die beruehrung elastischer koerper, J. Reine Angew. Math 92 (1881) 156171.
- [27] R. Mindlin, Compliance of elastic bodies in contact, Appl. Mech. 16 (1949) 259268.
- [28] M. Baniasadi, M. Baniasadi, B. Peters, Application of the extended discrete element method (xdem) in the melting of a single particle, AIP Conference Proceedings 1863 (1) (2017) 180003. arXiv:http://aip.scitation.org/doi/pdf/10.1063/1.4992363, doi:10.1063/1.4992363.
- [29] M. Mohseni, B. Peters, M. Baniasadi, Conversion analysis of a cylindrical biomass particle with a dem-cfd coupling approach, Case Studies in Thermal Engineering 10 (2017) 343 – 356. doi:https://doi.org/10.1016/j.csite.2017.08.004.
- [30] A. H. Mahmoudi, F. Hoffmann, B. Peters, Application of xdem as a novel approach to predict drying of a packed bed, International Journal of Thermal Sciences 75 (2014) 65–75.

- [31] W. E. Ranz, W. R. Marshall, Evaporation from drop, Chem. Engrg. Prog. 48 (3) (1952) 141–173.
- [32] S. Ergun, A. A. Orning, Fluid flow through randomly packed columns and fluidized beds, Industrial & Engineering Chemistry 41 (6) (1949) 1179–1184. arXiv:http://dx.doi.org/10.1021/ie50474a011, doi:10.1021/ie50474a011.
- [33] G. Pozzetti, B. Peters, On the choice of a phase interchange strategy for a multiscale DEM-VOF Method, AIP Conference Proceedings 1863. URL http://orbilu.uni.lu/handle/10993/28863
- [34] Peters, Bernhard, Pozzetti, Gabriele, Flow characteristics of metallic powder grains for additive manufacturing, EPJ Web Conf. 140 (2017) 13001. doi:10.1051/epjconf/201714013001.
 URL https://doi.org/10.1051/epjconf/201714013001
- [35] G. Pozzetti, B. Peters, A numerical approach for the evaluation of particle-induced erosion in an abrasive waterjet focusing tube, Powder Technology 333 (2018) 229 242. doi:https://doi.org/10.1016/j.powtec.2018.04.006.
- [36] T. Bakker, Softening in the blast furnace process: local melt formation as the trigger for softening of ironbearing burden materials, Ph.D. thesis, Delft University of Technology (1999).

- [37] A. Kemppainen, Limiting phenomena related to the use of iron ore pellets in a blast furnace, Ph.D. thesis, University of Oulu (2015).
- [38] A. Adema, Demcfd modelling of the ironmaking blast furnace, Ph.D. thesis, Delft University of Technology (2014).
- [39] P. F. Nogueira, R. J. Fruehan, Blast furnace burden softening and melting phenomena: Part i. pellet bulk interaction observation, Metallurgical and Materials Transactions B 35 (5) (2004) 829–838. doi:10.1007/s11663-004-0077-6.
- [40] A. Kemppainen, K. ichiro Ohno, M. Iljana, O. Mattila, T. Paananen, E.-P. Heikkinen, T. Maeda, K. Kunitomo, T. Fabritius, Softening behaviors of acid and olivine fluxed iron ore pellets in the cohesive zone of a blast furnace, ISIJ International advpub. doi:10.2355/isijinternational.ISIJINT-2015-023.
- [41] U. LEIMALM, M. LUNDGREN, L. S. KVIST, B. BJRKMAN, Off-gas dust in an experimental blast furnace part 1: Characterization of flue dust, sludge and shaft fines, ISIJ International, 50 (11) (2010) 1560– 1569.
- [42] M. Hallin, Bf inside story through quenching, in: John Floyd International Symposium on Sustainable Developments in Metals Processing, 2005.

- [43] Hallin, M., Hooey, L., Sterneland, J., Thulin, D., Lkab's experimental blast furnace and pellet development, Rev. Met. Paris 99 (4) (2002) 311-316. doi:10.1051/metal:2002204. URL https://doi.org/10.1051/metal:2002204
- [44] Z. Zhou, H. Zhu, A. Yu, B. Wright, P. Zulli, Discrete particle simulation of gassolid flow in a blast furnace, Computers & Chemical Engineering 32 (8) (2008) 1760 1772. doi:https://doi.org/10.1016/j.compchemeng.2007.08.018.
- [45] Z. Zhou, H. Zhu, A. Yu, P. Zulli, Numerical investigation of the transient multiphase flow in an ironmaking blast furnace, ISIJ International 50 (4) (2010) 515–523. doi:10.2355/isijinternational.50.515.
- [46] W. Yang, Discrete simulation of gas-solid flow and softening-melting behaviour in a blast furnace, Ph.D. thesis, The University of new south wales (2014).
- [47] T. V. Renard Chaigneau, J. Wise, Modern Blast Furnace Ironmaking, IOS Press BV, 2009.
- [48] E. Takegoshi, Y. Hirasawa, S. Imura, T. Shimazaki, Measurement of thermal properties of iron oxide pellets, International Journal of Thermophysics 5 (2) (1984) 219–228. doi:10.1007/BF00505502.
- [49] A. Kasai, T. Murayama, Y. Ono, Measurement of effective ther-

- mal conductivity of coke, ISIJ International 33 (6) (1993) 697–702. doi:10.2355/isijinternational.33.697.
- [50] G. Gustafsson, H. Hggblad, P. Jonsn, P. Marklund, Determination of bulk properties and fracture data for iron ore pellets using instrumented confined compression experiments, Powder Technology 241 (Supplement C) (2013) 19 – 27. doi:https://doi.org/10.1016/j.powtec.2013.02.030.
- [51] F. Hoffmann, Modelling heterogeneous reactions in packed beds and its application to the upper shaft of a blast furnace, Ph.D. thesis, University of Luxembourg (2014).
- [52] M. ASADA, Y. OMORI, Determination of young's modulus and poisson ratio of lump ores, Tetsu-to-Hagane 69 (7) (1983) 739–745.